QUANTIFICATION OF "DELIVERED" H_2 BY A VOLUMETRIC METHOD TO TEST H_2 STORAGE MATERIALS

Ilenia Rossetti[1*] and Gianguido Ramis[2]

[1] Dipartimento di Chimica, Università degli Studi di Milano, CNR-ISTM and INSTM Unit Milano-Università, v. C. Golgi 19, 20133 Milano, Italy

[2] Dipartimento di Ingegneria Civile, Chimica e Ambientale, Università degli Studi di Genova and INSTM Unit Genova-Università, P.le J.F. Kennedy 1, 16129 Genova, Italy

ABSTRACT

We set up and validated a volumetric method to quantify the amount of hydrogen "delivered" after saturation of a solid material as adsorber at different pressures (up to 100 kg_f/cm^2) and temperatures (down to 77 K). This is the practically most relevant datum to quantify the effectiveness of an adsorbent for the present application. A complementary dynamic method has been also developed to take into account the reversibility of adsorption and to assess in at least a semi-quantitative way the strength of interaction between H_2 and the adsorbent. The method has been applied to compare the hydrogen storage capacity of some significant different carbon-based materials (two active carbons and one graphite), as supplied or after thermal treatments under oxidising or reducing conditions. The best results, *ca*. 7 wt% H_2 "delivered", were achieved after saturation at 77 K, 20 kg_f/cm^2 with an active carbon with *ca.* 3000 m^2/g of apparent specific surface area. The thermal treatments, almost always inducing a drop in surface area, showed effective only for saturation at 273 K, in particular the oxidizing procedure. This was correlated to

* Corresponding author: email: ilenia.rossetti@unimi.it; fax: +39-02-50314300.

the formation of surface oxidized species, likely carboxylic groups, which improved the interaction strength between H_2 and the adsorbent.

Keywords: Hydrogen storage; Carbon based adsorbents; Active carbon; Graphite; Hydrogen adsorption.

1 – INTRODUCTION

The use of H_2 as fuel in conventional internal combustion engines or in fuel cells has the impressive advantage to form water as the only direct product, besides possessing the highest energy density among available fuels. However, the main problems in the growth of the so called “hydrogen economy” are represented by the development of efficient routes for its sustainable production, *i.e.* from renewable materials and energy sources, and of the methods to store and transport it in safe and suitable way for mobile applications. H_2 storage in carbon-based materials is indeed a still open issue, on one hand because of the lack of sufficiently effective materials to fulfil the current storage needs, on the other hand due to often unreliable data presented in the literature, or collected under practically irrelevant conditions.

The US Dept. of Energy (DoE) [1], circumscribed the most relevant goals for storage materials for on board transportation of hydrogen. Nevertheless, based on advances in car design and fuel cells technology, the above reported DOE targets have been recently revised in a less restrictive view [2]. Such properties refer to the entire storage system, including any auxiliary component and therefore the material should attain approximately twice the desired system capacity. It should be underlined that the newly adapted ultimate targets refer to a driving autonomy of 800 km for a medium size car, prescribing 5.5 wt% H_2 stored on board as gravimetric target for 2015 and 7.5 wt% as ultimate goal.

The critical properties of hydrogen storage materials to be evaluated for automotive applications are (i) light weight, (ii) cost and availability, (iii) high volumetric and gravimetric density of hydrogen, (iv) fast adsorption/desorption kinetics, (v) ease of activation, (vi) low temperature of dissociation or decomposition, (vii) appropriate thermodynamic properties, (viii) long-term cycling stability and (ix) high degree of reversibility [3-5].

From the reported data it appears that, even if not yet fulfilling the DOE targets, carbon based materials seem among the most promising for this application. Indeed, the highest and reproducible storage capacity has been reported for carbon-based sorbents, though with some contradictions.

Since H_2 adsorption is carried out under supercritical conditions, it adsorbs in the micropores and typically it may only lead to monolayer adsorption [6]. Physisorption is based on weak interactions and it becomes significant at very low temperature only. For example, the storage capacity of C-based materials decreases exponentially when passing from 77 K to r.t. Of course monolayer adsorption implies a linear relationship between capacity and surface area, though the phenomenon is completed by gas compression in the void space, which therefore turns out to be important.

Different methods were used to assess gas sorption capacity, classifiable into gravimetric, volumetric and TPD (temperature programmed desorption)-based procedures. Scarce accuracy in the determination of H_2 uptake may explain inconsistencies frequently found in the literature. All the cited methods present possible criticisms, for example the gravimetric one usually deals with a very low amount of solid [7-10]. TPD experiments share the problem of small sample size and often make use of mass spectrometric detectors, not well suited for the accurate quantification of H_2 adsorption/desorption [11-14]. Volumetric methods may be easily used at high pressure, but possible leaks, expansion problems and temperature effects may severely affect the measures. Furthermore, in most cases the term “volumetric” is misleading, since H_2 uptake is determined by measuring the pressure

difference before and after gas dosage over the sample. These should be better defined "manometric" methods.

Then, it appears that the set up of a simple and reliable method for the quantification of hydrogen storage properties is still an open issue. Therefore, the principal aim of the present work was to develop a very simple volumetric system to quantify the amount of hydrogen "delivered" from the sample after saturation, which is the most important practical parameter to evaluate the effectiveness of a hydrogen storage material. The method has been standardized under different operating conditions, to check its versatility and reliability. The method has been validated on two active carbons and one graphite, characterized by specific surface area (SSA) between 300 and 3000 m^2/g, in order to prove its applicability to widely different materials. A complementary dynamic testing procedure, based on the TPD technique, has been also developed to assess the reversibility of adsorption and its dynamics. The data have been elaborated according to very simple adsorption models, such as the Langmuir one. Finally, the results of an investigation on the effect of thermal treatments under reactive atmosphere over the above reported carbons and graphite are presented.

2 – EXPERIMENTAL

2.1 - Materials

The method has been set up and calibrated on three different carbon based materials, namely a superactivated carbon, kindly supplied by OSAKA GAS (type M30, *ca.*3000 m^2/g), an AC40 Acticarbon provided by CECA (*ca*. 1700 m^2/g) and a high SSA graphite (*ca.* 300 m^2/g). All the samples were supplied as fine powder, except Acticarbon AC40,

which was in form of *ca*. 3 mm diameter extrudates. Before testing it was ground and sieved into 0.15-0.25 mm particles.

Some thermal treatments under different atmospheres have been also attempted in order to tune up the textural properties of the carbons and to modify their surface composition. In particular, an oxidative treatment in flowing air at 723 K for 3h (OX) or a reducing treatment in H_2 flow at 723 K for 1 h (RED). After reduction the sample has been cooled in flowing nitrogen till r.t.

High purity H_2 (Sapio, pur. > 99.9995 vol%), He (Sapio, pur. > 99.9995 vol%), air (Sapio, pur. > 99.995 vol%) and N_2 (Sapio, pur. > 99.9995 vol%) were used for samples treatments and for both static and dynamic sorption/desorption tests.

2.2 – Materials characterisation

CHN analysis has been performed on a Thermo Finnigan EA 1112 instrument. Ash content was determined by thermal treatment in air at 1173 K until constant weight. X-ray diffraction analysis has been carried out on a Philips PW3020 diffractometer, by employing the Ni-filtred CuKα radiation. Patterns were collected in the range $20° \leq 2\theta \leq 80°$ with $2\theta = 0.02°$ steps (5 s/step).

Textural properties have been estimated from N_2 adsorption/desorption isotherms on a Micromeritics ASAP 2010 instrument after outgassing overnight at 573 K. Though not fully appropriate for the interpretation of microporous materials, the BET model has been used to calculate the SSA in order to compare the results with most literature data. Total pore volume has been determined at saturation ($P/P_0 = 0.995$) and the t-plot method has been used to determine the micropore volume.

FT-IR spectra (resolution 4 cm^{-1}) have been recorded with a Nicolet 6700 instrument. The analysis of the spectral region has been performed using KBr (FT-IR grade from Sigma-Aldrich) pressed disks (1 g with 1 wt% of carbon).

The Boehm titration method was also used to discriminate among different surface groups. The surface oxygen groups on carbons with acidic (carboxyl, lactone, phenol) as well as basic properties can be determined by titration. These groups differ in their acidities and can be distinguished by neutralisation with different solutions: HCl (for basic groups) and $NaHCO_3$, Na_2CO_3 and NaOH (for acidic groups). The acidic sites were determined by mixing *ca.* 0.1 g of carbon with 10 ml of different bases (0.1 M NaOH, 0.1 M $NaHCO_3$ or 0.05 M $NaCO_3$), left under agitation for 24 h. All the resulting solutions were then filtered and titrated with 0.05 M H_2SO_4. The basic sites were determined by mixing 0.1 g of material with 10 ml of 0.1 M HCl and the obtained solutions were titrated with 0.1 M NaOH.

2.3 – Volumetric H_2 storage tests

The apparatus, schematically sketched in Fig.1, is constituted of a sample holder, obtained from ¼" OD stainless steel tube (5 cm long), closed on one side and connected to a filter on the other side. The sample holder may be heated or cooled by a heater/cryostat, immersed in an ethylene-glycol bath or in a dewar flask containing either liquid nitrogen or any selected refrigerating mixture. Through a set of valves the material may be pretreated (outgassing by means of a vacuum pump during sample heating), or connected to the He gas line (determination of dead volume) or to the H_2 line (testing) at a selected gas pressure up to 100 kg_f/cm^2, indicated by a pressure indicator (PI).

After sample pretreatment under vacuum at 373 K for at least one hour, He is admitted at the selected testing pressure (up to 100 kg_f/cm^2) and temperature to determine the dead

volume and then the system is outgassed. H_2 is introduced in the sample holder at the same pressure and temperature, continuously adjusting pressure for at least 0.5 h.

After filling with the selected gas, the sample holder is closed and the apparatus is depressurised to ambient pressure. The amount of He or H_2 released is measured after elimination of the refrigerating unit and thermostating at r.t. The gas is allowed to freely expand by opening again the sample holder valve and its volume is measured at ambient temperature and pressure by means of a gas burette.

The conditions for outgassing and saturation were preliminarily repeatedly determined for each material till constancy of the results. Typically, the materials have been maintained at 273 K at H_2 relative pressure in the range 5 -100 kg_f/cm^2 and at 77 K between 5 and 20 kg_f/cm^2. Different amounts of every material have been tested, between 0.05 and 0.25g. For routine tests 0.10g were used.

Some analyses of the delivered H_2 have been carried out by pulsed injection into a mass spectrometer. No released impurities were observed.

2.3 – Dynamic adsorption tests

A conventional TPD apparatus, previously described in detail [15,16] has been used for the determination of H_2 uptake and release under dynamic conditions. The apparatus included 5 lines for gas feeding and it was equipped with a hot-wire detector (HWD). The sample, *ca.* 0.10 g, was placed in a U-shaped pyrex tube reactor and pretreated in flowing N_2 at 150°C for at least 0.5 h. This showed an appropriate pretreatment routine, as determined by some preliminary TPD runs for each material. The reactor may be by-passed in order to select different gaseous mixtures and to equilibrate with them the HWD detector. At the same time, the by-pass allows to thermally equilibrate the reactor as

desired. H_2 adsorption-desorption tests were carried out at atmospheric pressure and at 258-263 K.

3 – RESULTS AND DISCUSSION

3.1 – Materials characterisation

The three carbon based materials here analysed have been selected so to span a wide field of SSA values, form *ca*. 300 to *ca.* 3000 m^2/g (Table 1). Furthermore, the selection of two active carbons and one graphite allowed to evaluate the effect of carbon structure on the sorption properties.

According to XRD analysis, here not reported, both the OSAKA GAS and CECA AC40 active carbons (ACs) showed completely amorphous, whereas the diffractogram of the third sample revealed a pure graphitic structure. The diffractograms did not modify after any of the proposed thermal treatments.

The textural properties of each sample are reported in Table 1. For both the as supplied ACs, microporosity mainly contributed to the total SSA. The mean pore size showed between 2.0 and 3.5 nm, values higher by one order of magnitude with respect to the kinetic diameter estimated for hydrogen [17]. By contrast, the graphite sample showed much lower SSA and pore volume with respect to ACs, with a poor contribution of microporosity. The mean pore size was accordingly higher, *ca*. 8 nm.

It should be noticed, as recalled in the Introduction, that H_2 adsorbs under supercritical conditions [6] even when the tests are carried out at 77 K, thus leading to monolayer coverage only. Therefore, the pore size should be sufficiently large to avoid diffusional limitations, but at the same time too much void space would depress the overall storage capacity [18-22].

For every material the oxidative treatment induced a higher weight loss than the reducing one (Table 2), but the effect was different for the three samples. The AC with the highest SSA showed more prone to oxidation and reduction, followed by graphite and finally by the AC40 carbon. The reducing treatment induced for both ACs a 20-25% contraction of the SSA, to be compared with a 27-33% induced by oxidation. The effect of air treatment on graphite was very similar and provoked a substantial loss of microporosity. By contrast, a slight increase of SSA and microporosity, with consequent decrease of the mean pore size, was achieved after reduction. This may be explained by the formation of surface defects on the graphite planes. As indirect confirmation, the weight loss of this sample was proportionally higher than that achieved after reduction of other samples.

The CHN composition was also determined (Table 2). The commercial extrudates of AC40 showed the highest ash content, the graphite the lowest. Oxygen content may be roughly estimated by difference from the total weight. For both the ACs the composition widely varied following each treatment, especially the M30 sample, which confirmed less stable than AC40. Reduction brought about an increase of C and H content, likely eliminating oxidised functions of carbon surface. The opposite, of course, occurred after oxidation. Some nitrogen containing functions may be introduced due to high temperature interaction with N_2 (from air or during flushing).

In order to get further data regarding the effect of treatments under oxidising or reducing conditions, vibrational analysis of the active carbon has been performed. IR spectroscopy, in its various forms, is an important and forceful technique which can give information about structures, such as the surface functional groups, and can provide basic spectra of the activated carbon for comparison with spectra of the same carbon-containing adsorbed species [23]. The infrared spectra of KBr pressed disks of some representative samples are presented in Fig. 2. According to the tendency to absorb most of the radiation, the spectra of all the sample were characterised by a very low transmittance. Nevertheless, in

the spectrum of the Osaka Gas OX sample some weak, but significant, bands can be observed near 3430, 1725, 1600 and 1220 cm^{-1}, as better evidenced in Fig. 3. Such bands are attributable to O-H stretching, C=O stretching, O-H deformation and C-O stretching, respectively. This is in good agreement with the presence of surface carboxyl structures [24,25]. However, we cannot exclude the presence of water to explain the bands at 3430 and 1600 cm^{-1}. All these bands were absent in the same sample treated in H_2 (Osaka Gas RED). Even if oxidised under the same conditions, samples CECA AC40 OX and CECA AC40 RED gave rise to very poor, almost undetectable bands, due to their much lower surface area than the previously reported samples, which leads to lower concentration of relevant surface species. The same holds for the graphite-based samples, not reported for brevity.

The Boehm titration is a commonly used technique to determine the acidic oxygen surface functional groups on carbon samples, since bases of different strength ($NaHCO_3$, Na_2CO_3 and NaOH) may neutralize different acidic oxygen surface functionalities [26,27]. The weakest base, $NaHCO_3$, neutralizes only the strongest acidic carbon surface functionalities, which are the carboxylic groups. By contrast, Na_2CO_3 neutralizes both carboxylic and lactonic groups, while the strongest base, NaOH, neutralizes every acidic functionality, *i.e.* carboxylic, lactonic and phenolic groups. The number of each type of surface group can be determined by difference between the uptake of each reaction base. The surface sites with basic character may be quantified as well by neutralisation with HCl. The results for some representative samples are reported in Table 3.

The amount of surface species determined is in accordance with the conclusions of CHN and IR analyses. The amount of surface sites having basic character was lower with respect to those with acidic nature. The highest concentration was observed with sample Osaka Gas. As expected, the oxidising treatment increased (*ca*. doubled) the amount of carboxylic and phenolic surface groups, the latter being the most abundant species. By

contrast, lactonic functionalities were not formed with oxidising treatment. Nevertheless, lactonic groups were almost completely abated by reduction, which left practically unaffected the concentration of carboxylic and phenolic functions. Surface groups with basic character remained substantially unchanged after oxidation or reduction.

3.2 – Volumetric H_2 storage tests

Preliminary blank tests have been carried out for the calibration of the instrument. The dead volume of the apparatus (from the sample holder valve to the gas burette) has been calibrated with both He and H_2. By contrast, the dead volume including the sample holder was measured for each sample with He under the appropriate testing conditions. Blank tests repeated with He and H_2 revealed that the dead volume at ambient pressure and temperature was the same.

Nevertheless, scarcely reproducible data have been obtained if the immersion level of the sample holder in the refrigerating mixture changed, especially under cryogenic conditions. Therefore, the system was calibrated by keeping rigorously constant the refrigerant level on the sample holder and by carefully insulating its external portion.

Sample pretreatment has been carried out under vacuum at different temperatures and for different times. Typically, 373 K for 1 h allowed to obtain reproducible results. Accordingly, a proper saturation time was selected.

Each sorption cycle has been repeated at least 5 times under every operating condition, more in case of unreliable results, *i.e*. deviating from the mean value by more than 3 times the standard deviation. In such cases, sporadically, further readings were added to obtain at least 5 reliable data. During the setting up of the method, repeated tests with different batches have been carried out to check the repeatability of the whole procedure. Table 4

and 5 represent the mean values and standard deviation of H_2 delivered after saturation at different temperature for every sample.

The volume of H_2 adsorbed ranged typically between 5 and 150% of the dead volume, which was measured with maximum relative error up to 0.8%.

3.2.1 – Adsorption tests at 273 K

The amount of delivered H_2 increased as expected with increasing the saturation pressure and was higher when adsorption was conducted at lower temperature.

As for adsorption at 273 K on the as supplied samples, the storage capacity was roughly proportional to the SSA and porosity of the material. After treatment under either oxidising or reducing conditions, very small differences of H_2 sorption capacity was obtained. Indeed, such treatments did not induce any substantial modification of the composition of the material, but only a similar decrease of SSA. Though the effect on SSA was limited in the case of treated graphite, a bit more marked difference in composition was achieved, reflecting in differences in sorption capacity. In particular, in the case of graphite both treatments induced a marked increase of storage capacity. The reducing treatment induced the formation of defects in the graphitic layers with a 10% increase of SSA. By contrast, the decrease of SSA observed after oxidation was likely compensated by the availability of oxidised surface functions (see Tables 2 and 3) which acted as favourable adsorption sites for H_2. Nevertheless, the best results were achieved with reduction and, particularly, with reducing treatments over the very high SSA AC from Osaka Gas. Even if in both cases a lower SSA was available, the formation of lower coordination defective sites (reduction) and of oxidised surface functional groups, mainly of lactonic nature, strongly improved the sorption capacity at 273K.

3.2.2 – Adsorption tests at 77 K

When turning our attention to adsorption at 77 K, a much higher storage capacity was observed even at 20 bar only, a much lower pressure than what often reported in the literature [17,28-30]. *Ca*. 7 wt% delivered H_2 has been measured for the as supplied Osaka Gas material and also in this case the capacity decreased with decreasing SSA. However, at difference from tests at 273 K, the effect of any treatment under reacting conditions was poor if not even detrimental. During adsorption at 77 K, the thermal energy of the H_2 molecule is reasonably low to account for its adsorption rather irrespectively of the surface sites composition. So the most important factor governing adsorption seems surface sites availability, *i.e*. high SSA. By contrast, at 273 K, adsorbent-adsorbate interaction is by far much weaker, so tuning surface composition may help to increase adsorption capacity.

3.2.3 – General comments on the testing method

By looking at the data reported in Tables 4 and 5, one may conclude that the method is reliable and reproducible for different batches of materials. The differences calculated on at least 5 repeated load / unload cycles were almost always lower than 10%, of course decreasing with increasing the measured value, rendering more precise the evaluation of the performance of the best sorption materials. No significant effect of sample amount (above 0.05 g) or particle size was ever noticed.

A comprehensive review of the possible failure modes during the quantification of H_2 sorption properties addressed many topics [31]. Starting from criticized data reported for single walled nanotubes (SWNTs), apparently adsorbing up to 10 wt% [32] and carbon nanofibers (CNFs), even up to 67.55 wt% [33], possible error sources have been reviewed. Volumetric and manometric measurements are usually better than gravimetric ones, due to more standardized apparatus and better temperature and pressure control. A critical correction needed for the latter is buoyancy, while for the former is the correct

determination of dead volume. This parameter is usually detected with He, though assumptions may fail that it does not adsorb at all on the sample and that it can adequately “see” the volume as H_2 does [34-36].

Some IUPAC guidelines developed for gas adsorption (BET method) have been extended also to H_2 storage. Apart from general aspects such as proper system calibration, an accurate determination of temperature and pressure, absence of leaks, other keypoints should be taken into account. One is the possible thermal effect during adsorption, particularly relevant for hydrides, imposing to wait till thermal re-equilibration after gas dosage. A sufficient time to reach equilibrium should be waited and in case an accurate inspection of the isotherm may reveal problems from this point of view. This is particularly relevant when diffusion through micropores is at the basis of the phenomenon. Some dependence on sample size has also been reported, particularly for very high SSA materials (*e.g*. for ACs), indicating that the best compromise is a total available surface area of 20-50 m^2 in the sample holder. However, care should be taken when SSA is very high, in order to avoid weighting errors and in every case not less than 50 mg should be considered for testing [37]. High gas purity is also required (> 99.999%), providing filter/traps along the feeding lines. Another point is the volume to sample mass ratio, which would affect the determination of the dead volume. Sample outgassing should be done at sufficiently low pressure to allow cleaning, but not to introduce defects on the sample surface. Furthermore, the pretreatment temperature may affect performance, especially for ACs. Another very critical point is the pressure correction with appropriate equations of state (EOS) to account for deviations from ideal gas properties. This is an open issue, since some of the most reliable models up to now used for data correction, the Soave–Redlich–Kwong (SRK) and Benedict–Webb–Rubin (BWR) equations, are hardly useful in the temperature and pressure ranges of most of the reported tests. Even when testing the

samples below ambient pressure (P < 15 Pa) corrections may be needed due to the so-called thermal transpiration effect.

The presently proposed method overcomes most of these problems. Particularly, as above recalled, one critical point during the elaboration of storage data at high pressure is the need to select proper EOS to correctly define gas properties at high pressure or low temperature [37]. This point could however be skipped, because H_2 is stored at the desired pressure and temperature, but no direct quantification under these conditions is given. The amount of hydrogen released (delivered) by the sample, has been indeed quantified in our apparatus under ambient operating conditions. The quantification of delivered H_2 represents a good advantage, since some irreversibility during hydrogen uptake may occur and the important datum for practical application is only the amount of H_2 actually released from the storage tank for use.

Another advantage of the here proposed apparatus is its versatility. For safety reasons, due to the materials selected and to the design of the sample holder, the maximum operating pressure was 100 bar during testing at 273 K and 20 bar at 77 K. However, minor modifications would allow an increase of such parameters, as well as the selection of different refrigerating mixtures.

3.3 – Dynamic H_2 adsorption/desorption tests

A further adsorption/desorption test has been also set up in order to better assess the dynamics and reversibility of hydrogen storage and release. By means of this test we also attempted to assess semi-quantitatively the strength of interaction between H_2 and the adsorber surface.

After optimisation, heating at 130°C under inert gas flow for 1 h proved an effective procedure to clean up the sample. Then, the reactor is by-passed and after cooling at r.t.,

the reactor is immersed in a refrigerating bath, setting sample temperature at 258-263 K. A 10 vol% H_2/N_2 gas mixture is fed to the HWD detector through the by-passing line and once the base line is stable and the sample temperature is set to the desired value, the gas is admitted through the reactor. H_2 consumption due to adsorption is monitored and after the baseline returns to the initial value the gas is excluded from the reactor and sent to the detector through the bypass.

In order to quantify hydrogen desorption, pure N_2 is set as carrier gas through the by-pass and the refrigerating bath is eliminated, allowing the closed reactor to reach r.t.. When the baseline reaches again the stable initial value and the temperature of the reactor is equilibrated, the pure carrier gas is allowed into the reactor, the latter is heated up to 500°C (10°C/min) and the H_2 desorption peak is registered.

The results of this set of tests are reported in Table 6. The reversibility of the sorption/desorption process is confirmed by the very similar areas of the sorption/desorption peaks.

The TPD of adsorbed H_2 also allowed to compare the temperature range in which desorption occurred for different materials. By looking at Table 6, the CECA AC40 material released H_2 in a very narrow region at low desorption temperature. Nevertheless its mean pore size was comparable with that of the Osaka Gas sample, which instead showed much broader and high temperature TPD peak. On the other hand, both the reduced and oxidised Osaka Gas samples were characterised by wider average pore size than other samples, though leading to broad and high temperature desorption peaks. Hence, the influence of pore size, *i.e*. of possible diffusional limitations, on the shape of the TPD peak was substantially ruled out.

Therefore, the main parameter determining the desorption temperature is the interaction strength between the adsorbate and the substrate. Furthermore, a broad peak may suggest heterogeneity of adsorption sites. Thus, by comparing the different materials

families from this point of view one may conclude that the CECA AC40 carbon leads to weak adsorption, irrespectively of the treatment; intermediate strength and a bit higher heterogeneity characterises the graphite-based samples, whereas higher adsorption strength and much higher heterogeneity is found for Osaka Gas samples, especially after treatments under oxidising or reducing atmosphere. These results, together with the determination of surface groups may help in explaining the adsorption behaviour of the volumetric tests.

3.4 – Data elaboration through the Langmuir equation

The adsorption data collected at different pressure were preliminarily elaborated through the Langmuir model. Though this is a very simple equation to describe adsorption, it may be adapted to the present case since H_2 may lead up to a monostrate. The Langmuir equation was linearised in the following form and adapted to our data:

$$\frac{P}{n_{ads}} = \frac{P}{n_{mono}} + \frac{1}{n_{mono} \cdot K_{ads}}$$

where P is the adsorption pressure and n_{ads} the moles of H_2 adsorbed per g of sample (experimental data), whereas n_{mono} and K_{ads} are the moles of H_2 leading to an adsorbed monolayer and the equilibrium adsorption constant, respectively, to be determined from data regression. Actually, our experimental data refer to the amount of H_2 released, but the reversibility of adsorption and testing under dynamic conditions allowed to conclude that the amount of hydrogen released is representative, at least for this set of samples, of the amount adsorbed.

Both the parameters obtained from the application of the Langmuir model may be of interest to interpret our volumetric adsorption data. The calculated equilibrium constant may indeed be an index for internal comparison to understand how favoured was adsorption. On the other hand, the calculation of the amount of H_2 corresponding to a monostrate may be used to calculate the coverage degree. The latter gives an indication on the surface still available for adsorption and suggests the feasibility of further adsorption by enhancement of pressure, as better detailed in the following.

The results of this calculation are reported in Table 7. As for the data collected after adsorption at 273K, the calculated n_{mono} varied in rough agreement with SSA. Moreover, the K_{ads} values increased for each set of samples after treatment under oxidising or reducing conditions. Higher equilibrium constant were achieved with the best performing materials. This, together with high SSA ensured the best material performance. In the last column of Table 7 the values of the coverage degree attained after adsorption at 100 kg_f/cm^2 are reported for each material, calculated as:

$$\theta = \frac{n_{ads}}{n_{mono}}$$

This parameter may be taken as an indication of the further potentiality of the material. For instance, the behaviour of the three CECA AC40 samples is very similar and the coverage degree below 0.5 may suggest a further enhancement of the operating pressure (if economically and technically feasible) to improve the sorption capacity. By contrast, the available surface of the as supplied graphite or of the oxidised Osaka Gas samples is almost completely filled. This discourages an enhancement of pressure, which would bring about only a limited added value.

4 - CONCLUSIONS

A volumetric method for the measurement of H_2 storage capacity in terms of delivered hydrogen has been set up. Data showed reproducible within a 10% error and the present system allowed the investigation of the materials up to 100 kg_f/cm^2 and at different temperatures down to 77 K.

The system has been validated by comparing different carbon based materials, with BET SSA ranging from 300 to 3000 m^2/g. The amount of H_2 released after saturation at 77 K showed mainly dependent on SSA, physisorption being sufficiently strong, irrespectively of the nature of surface sites. SSA showed important also during adsorption at 273 K, but in this case the presence of surface defects or of oxidised groups, forming upon thermal treatment under reducing or oxidising atmosphere, improved in most cases the sorption capacity of the material.

The dynamics of H_2 adsorption/desorption was also analysed by setting up a different testing procedure to compare the amount of H_2 loaded and delivered under flowing conditions. Storage was reversible for all the materials, but the form and temperature range of the desorption peak showed dependent on the sorbent/sorbate interaction strength. The best performing samples during static volumetric testing were characterised by higher desorption temperature, indicating more effective interaction.

The best results*, i.e. ca*. 7 wt% H_2 delivered after adsorption at 77 K and 20 kg_f/cm^2, have been attained with the as-supplied AC with 3000 m^2/g surface area. Oxidation of the same material was beneficial when testing at 273 K, allowing to obtain *ca*. 2.6 wt% H_2 delivered after saturation at 100 kg_f/cm^2. This was attributed to the formation of surface oxidised species, likely carboxylic groups, which showed effective in increasing the interaction strength between hydrogen and the sorbent surface. This was particularly important during adsorption at relatively high temperature (273 K), since at this temperature the thermal energy of the adsorbing molecule is much higher and only a stronger interaction with the surface may lead to sufficiently stable adsorption.

ACKNOWLEDGEMENTS

The authors kindly thank Osaka Gas Co. Ltd. (Dr. M. Yoshikawa) for supplying AC samples. The valuable help of the MoS graduating students P. Poma, A. Del Regno, V. Radaelli and E. Cavo in collecting the experimental data is gratefully acknowledged.

REFERENCES

1. www.doe.gov
2. Yang J, Sudik A, Wolverton C, Siegel DJ. High capacity hydrogen storage materials: attributes for automotive applications and techniques for materials discovery. Chem Soc Rev 2010;39:656-675.
3. Niemann MU, Srinivasan SS, Phani AR, Kumar A, Goswami DY, Stefanakos EK. Room temperature reversible hydrogen storage in polyaniline (PANI) nanofibers. J Nanosci and Nanotech 2009;9:4561-4565.
4. Lim KL, Kazemian H, Yaakob Z, Ramli Wan Daud W. Solid-state Materials and Methods for Hydrogen Storage: A Critical Review. Chem Eng Technol 2010;33: 213-226.
5. Rossetti I. Micro and nanostructured materials for H_2 storage: Application to mobile fuel cell systems. Micro and Nanosystems 2011;3:331-347.
6. Zhou L. Progress and problems in hydrogen storage methods. Renew Sust Energy Rev 2005;9:395-408.
7. Chen Y, Shaw DT, Bai XD, Wang EG, Lund C, Lu WM, Chung DDL. Hydrogen storage in aligned carbon nanotubes. Appl Phys Lett 2001;78:2128-2130.

8. Strobel R, Jorissen L, Schliermann T, Trapp V, Schutz W, Bohmhammel K, Wolf G, Garche J. Hydrogen adsorption on carbon materials. J Power Sources 1999;84:221-224.
9. de la Casa-Lillo MA, Lamari-Darkrim F, Cazorla-Amoros D, Linares-Solano A. Hydrogen Storage in Activated Carbons and Activated Carbon Fibers, J Phys Chem B 2002;106:10930-10934.
10. Hanada K, Shiono H, Matsuzaki K. Hydrogen uptake of carbon nanofibers under moderate temperature and low pressure. Diam Relat Mater 2003;12:874-877.
11. Bai XD, Zhong DY, Zhang GY, Ma XC, Liu S, Wang EG, Chen Y, Shaw David T. Hydrogen storage in carbon nitride nanobells. Appl Phys Lett 2001;79:1552-1554.
12. Shiraishi M, Takenobu T, Yamada A, Ata M, Kataura H. Hydrogen storage in single-walled carbon nanotube bundles and peapods. Chem Phys Lett 2002;358:213-218.
13. Ritschel M, Uhlemann M, Gutfleisch O, Leonhardt A, Graff A, Taschner C, Fink J. Hydrogen storage in different carbon nanostructures. Appl Phys Lett 2002;80:2985-2987.
14. Orimo S, Matsushima T, Fujii H, Fukunaga T, Majer G. Hydrogen desorption property of mechanically prepared nanostructured graphite. J Appl Phys 2001;90:1545-1549.
15. Rossetti I, Pernicone N, Forni L. Characterisation of Ru/C catalysts for ammonia synthesis by oxygen chemisorption. Appl Catal A: General 2003;248:97-103.
16. Rossetti I, Biffi C, Forni L. Oxygen non-stoichiometry in perovskitic catalysts: Impact on activity for the flameless combustion of methane. Chem Eng J 2010;162:768-775.
17. Alcaniz-Monge J, Román-Martínez MC. Upper limit of hydrogen adsorption on activated carbons at room temperature: A thermodynamic approach to understand

the hydrogen adsorption on microporous carbons. Micropor Mesopor Mater 2008;112:510-520.

18. Kowalczyk P, Holyst R, Terzyk AP, Gauden PA. State of Hydrogen in Idealized Carbon Slitlike Nanopores at 77 K. Langmuir 2006;22:1970-1972.
19. Rzepka M, Lamp P, de la Casa-Lillo MA. Physisorption of hydrogen on microporous carbon and carbon nanotubes. J Phys Chem B 1998;102:10894-10898.
20. Kowalczyk P, Tanaka H, Holyst R, Kaneko K, Ohmori T, Miyamoto J. Storage of hydrogen at 303 K in graphite slitlike pores from grand canonical Monte Carlo simulation. J Phys Chem B 2005;109:17174-17183.
21. Patchkovskii S, Tse JS, Yurchenko SN, Zhechkov L, Heine T, Seifert G. Graphene nanostructures as tunable storage media for molecular hydrogen. Proc Nat Acad Sci 2005;102:10439-10444.
22. Georgiev PA, Ross DK, Albers P, Ramírez-Cuesta AJ. The rotational and translational dynamics of molecular hydrogen physisorbed in activated carbon: a direct probe of microporosity and hydrogen storage performance. Carbon 2006;44:2724-2738.
23. Bansal RP, Donnet JP, Stoeckli F. Active Carbon. Marcel Dekker (New York), 1988, 67-92.
24. Stobinski L, Lesiak B, Zemek J, Jiricek P, Biniak S, Trykowski G. Studies of oxidized carbon nanotubes in temperature range RT–630 °C by the infrared and electron spectroscopies. J Alloys and Compounds 2010;505:379-384.
25. Geng W, Nakajima T, Takanashi H, Ohki A. Analysis of carboxyl group in coal and coal aromaticity by Fourier transform infrared (FT-IR) spectrometry. Fuel 2009;88:139-144.

26. Goertzen SL, Thériault KD., Oickle AM, Tarasuk AC, Andreas HA. Standardization of the Boehm titration. Part I. CO_2 expulsion and endpoint determination. Carbon 2010; 48:1252-1261.
27. Oickle AM, Goertzen SL, Hopper KR, Abdalla YO, Andreas HA. Standardization of the Boehm titration: Part II. Method of agitation, effect of filtering and dilute titrant. Carbon 2010;48:2213-3322.
28. Zubizarreta L, Menéndez JA, Job N, Marco-Lozar JP, Pirard JP, Pis JJ, Linares-Solano A, Cazorla-Amorós D, Arenillas A. Ni-doped carbon xerogels for H_2 storage. Carbon 2010;48:2722-2733.
29. Ioannatos GE, Verykios XE. H_2 storage on single- and multi-walled carbon nanotubes. Int J Hydrogen Energy 2010;35:622-628.
30. Jiménez V, Sánchez P, Díaz JA, Valverde JL, Romero A. Hydrogen storage capacity on different carbon materials. Chem Phys Lett 2010;485:152-155.
31. Broom DP. The accuracy of hydrogen sorption measurements on potential storage materials. Int J Hydrogen Energy 2007;32:4871-4888.
32. Dillon CA, Jones KM, Bekkedahl TA, Kiang CH, Bethune DS, Heben MJ. Storage of hydrogen in single-walled carbon nanotubes. Nature 1997;386:377-379.
33. Chambers A, Park C, Baker RTK, Rodriguez NM. Hydrogen storage in graphite nanofibers. J Phys Chem B 1998;102:4253-4256.
34. Neimark AV, Ravikovitch PI. Calibration of pore volume in adsorption experiments and theoretical models. Langmuir 1997;13:5148-5160.
35. Malbrunot P, Vidal D, Vermesse J, Chahine R, Bose TK. Adsorbent helium density measurement and its effect on adsorption isotherms at high pressure. Langmuir 1997;13:539-544.
36. Sircar S. Measurement of Gibbsian Surface Excess. AIChE J 2001;47:1170.

37. Rouquérol F, Rouquérol J, Sing K. Adsorption by powders and porous solids: principles, methodology and applications, Academic Press, London, 1999.

Table 1: Textural properties of the materials used. SSA = Specific Surface Area.

Sample	SSA BET (m^2/g)	SSA Langmuir (m^2/g)	Total pore volume* (cm^3/g)	Micropore volume** (cm^3/g)	Micropore Area** (m^2/g)	Mean pore size (Å)
Osaka Gas	3059	4456	1,82	1,70	2998	24
Osaka Gas RED	2440	2485	2,01	1,90	2380	33
Osaka Gas OX	2074	2283	1,72	1,62	2019	33
CECA AC40	1736	3255	1,09	0,89	1082	25
CECA AC40 RED	1313	1771	0,70	0,62	1260	22
CECA AC40 OX	1274	1728	0,71	0,63	1180	22
Graphite	291	341	0,49	0,03	61	82
Graphite RED	325	448	0,47	0,08	158	58
Graphite OX	200	281	0,41	0,01	11	82

* Measured at P/P_0 = 0.995

** Determined from t-plot

Table 2: Effect of thermal treatments and elemental analysis. ΔW% = weight loss due to the treatment.

Sample	**ΔW%**	**C (wt%)**	**H (wt%)**	**N (wt%)**	**Ash (wt%)**
Osaka Gas	/	90.58	0.23	0.00	6
Osaka Gas RED	-8,53	93.34	0.09	0.08	/
Osaka Gas OX	-28,66	83.06	0.31	0.20	/
CECA AC40	/	82.76	0.93	0.24	9
CECA AC40 RED	-1,46	83.26	0.87	0.29	/
CECA AC40 OX	-4,25	81.76	0.64	0.32	/
Graphite	/	95.02	0.08	0.30	1
Graphite RED	-4,82	98.74	0.53	0.21	/
Graphite OX	-9,23	97.17	0.59	0.23	/

Table 3: Boehm titration of different surface groups.

	Acidic groups (mmol/g_{carbon})			Basic groups (mmol/g_{carbon})
Sample	Cabox.	Lactonic	Phenolic	
Osaka Gas	0.55	0.64	1.22	0.89
CECA AC40	0.37	0.40	0.85	0.40
Graphite	0.66	-	0.98	0.93
Osaka Gas RED	0.51	0.02	1.36	0.89
Osaka Gas OX	0.94	0.67	3.06	0.98

Table 4: H_2 delivered for each sample. Adsorption temperature 273 K at selected different pressures.

	H_2 wt% delivered after adsorption at 273 K		
Sample	P = 20 [kg_f/cm^2]	P = 40 [kg_f/cm^2]	P = 100 [kg_f/cm^2]
Osaka Gas	0.28 ± 0.12	0.48 ± 0.04	1.04 ± 0.14
Osaka Gas RED	0.60 ± 0.16	0.94 ± 0.13	1.8 ± 0.2
Osaka Gas OX	0.9 ± 0.2	1.29 ± 0.05	2.6 ± 0.2
CECA AC40	0.23 ± 0.09	0.65 ± 0.14	0.77 ± 0.27
CECA AC40 RED	0.33 ± 0.03	0.67 ± 0.14	1.02 ± 0.13
CECA AC40 OX	0.27 ± 0.04	0.54 ± 0.10	0.92 ± 0.18
Graphite	0.14 ± 0.01	0.17 ± 0.04	0.17 ± 0.02
Graphite RED	0.22 ± 0.14	0.41 ± 0.04	1.43 ± 0.17
Graphite OX	0.34 ± 0.09	0.48 ± 0.17	1.46 ± 0.17

Table 5: H_2 delivered for each sample. Adsorption temperature 77 K at selected different pressures. The sample Osaka Gas RED was also tested at 10 kg_f/cm^2 and 15 kg_f/cm^2 leading to 4.8 ± 0.3 and 5.89 ± 0.11 wt% H_2 delivered, respectively.

	H_2 wt% delivered after adsorption at 77 K	
Sample	P = 5 [kg_f/cm^2]	P = 20 [kg_f/cm^2]
Osaka Gas	3.3 ± 0.6	6.9 ± 0.3
Osaka Gas RED	3.5 ± 0.2	6.6 ± 0.2
Osaka Gas OX	2.8 ± 0.3	3.7 ± 0.1
CECA AC40	1.85 ± 0.18	4.2 ± 0.3
CECA AC40 RED	2.21 ± 0.06	4.92 ± 0.12
CECA AC40 OX	1.3 ± 0.2	1.8 ± 0.1
Graphite	0.69 ± 0.05	1.91 ± 0.03
Graphite RED	0.71 ± 0.03	0.8 ± 0.1
Graphite OX	0.23 ± 0.05	0.31 ± 0.07

Table 6: Dynamic adsorption/desorption results.

Sample	**Ads. peak area (mV•s)**	**Des. Peak area (mV•s)**	**T range des. peak (°C)**
Osaka Gas	8047	8044	200-300
Osaka Gas RED	13704	13701	160-400
Osaka Gas OX	2303	2312	110-410
CECA AC40	2146	2148	25-35
CECA AC40 RED	5105	5112	35-50
CECA AC40 OX	6647	6652	25-40
Graphite	2826	2828	50-70
Graphite RED	9062	9059	65-180
Graphite OX	2506	2507	35-115

Table 7: Coverage degree at the maximum saturation pressure and equilibrium constant as determined from the Langmuir model. Adsorption temperature 273 K.

Sample	$\mathbf{n_{mono}}$ **(mol/g)**	$\mathbf{K_{ads}}$ **(cm^2/kg_f)**	**θ**
Osaka Gas	0.018	0.0040	0.29
Osaka Gas RED	0.019	0.0089	0.48
Osaka Gas OX	0.016	0.0092	0.85
CECA AC40	0.013	0.0067	0.40
CECA AC40 RED	0.011	0.0090	0.47
CECA AC40 OX	0.011	0.0068	0.40
Graphite	0.001	0.0050	0.81
Graphite RED	0.004	0.0062	0.40
Graphite OX	0.003	0.0060	0.51

Fig. 1: Sketch of the volumetric apparatus set up for H_2 sorption tests.

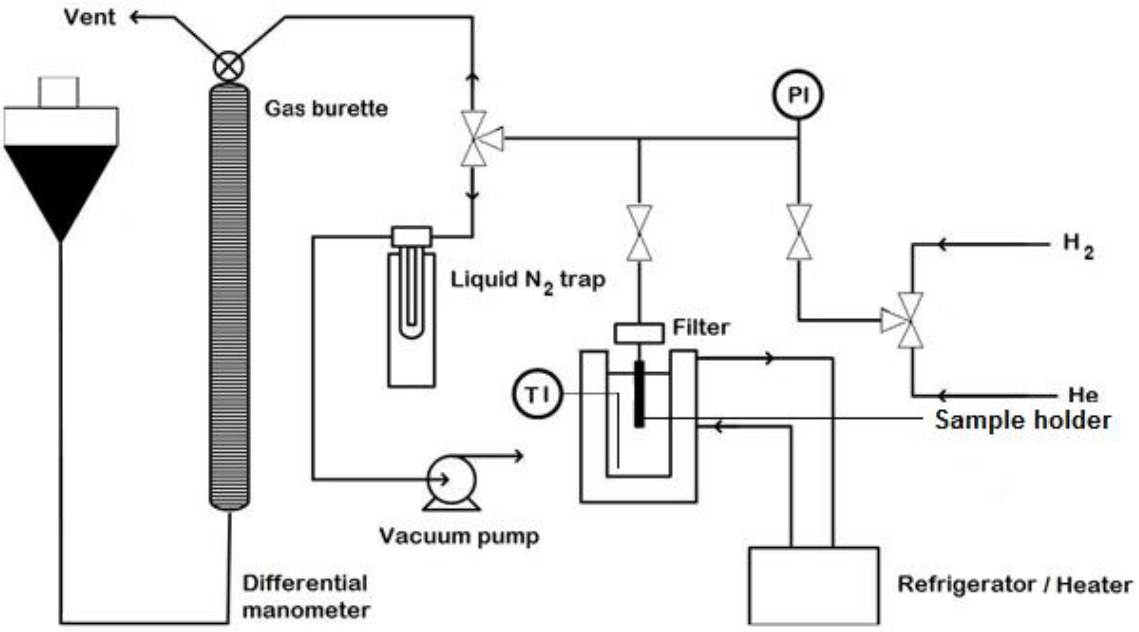

Fig. 2: FT-IR spectra of samples a) Osaka Gas RED, b) Osaka gas OX, c) CECA AC40 RED and d) CECA AC40 OX.

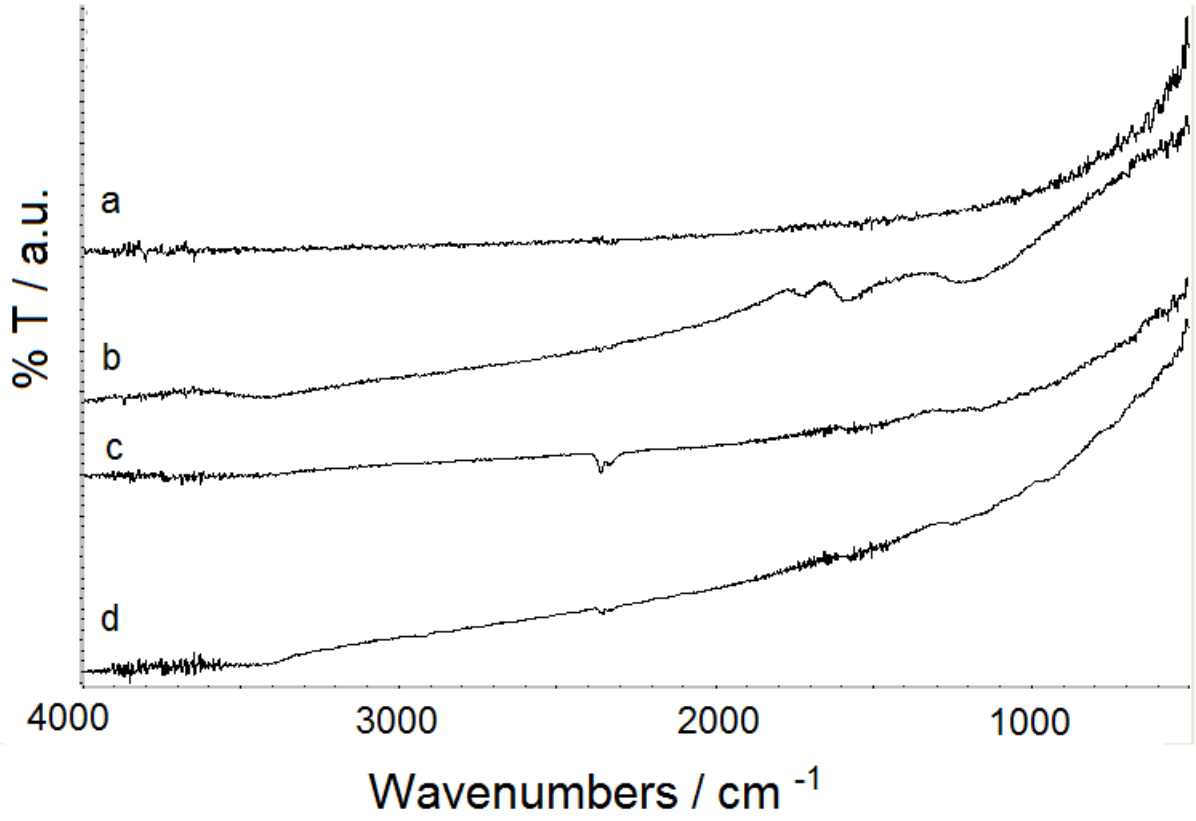

Fig. 3: FT-IR spectra (800-2000 cm^{-1} region) of samples a) Osaka Gas RED, b) Osaka gas OX, c) CECA AC40 RED and d) CECA AC40 OX.